MODULATION OF CONVENTIONAL TV SIGNALS IN ALL-DIGITAL CATV NETWORK HEAD ENDS

Dietmar Wenzel and Joachim Speidel
Institute of Telecommunications
University of Stuttgart
Pfaffenwaldring 47, D-70569 Stuttgart, Germany

ABSTRACT

In this paper, a new digital intermediate frequency modulator for conventional TV signals using digital signal processing is presented. A composite colour video signal and two associated audio signals are converted into a digital composite TV signal with spectrum at intermediate frequency. The modulator is designed for the high quality requirements that exist in professional equipment for CATV head ends. The architecture of the digital modulator shown is optimized for an implementation with ASICs. The signal processing with reduced complexity is described in detail, the structures and the design of the filters are illustrated and the simulated results are presented.

1. INTRODUCTION

Up to now most CATV networks have been using analog electrical or optical transmission techniques to distribute TV and FM audio programs to subscribers within a wide area. Usually, the networks are divided into several distribution areas each having a separate head end that works independently. The frequency division multiplexed signal (FDM) containing the separately supplied TV channels is generated by analog mixers and filters. These systems suffer from distortion, noise and temperature drift effects caused by the physical characteristics of amplifiers, oscillators and filters.

Today, digital optical transmission systems with bit rates of 10 Gbit/s and beyond are commercially available. Thus, it is possible to transmit the entire digitized CATV signal with a bandwidth up to 860 MHz as a digital signal with a resolution of 12 bit in an optical fiber [1, 2], e.g., an SDH optical transmission system (SDH synchronous digital hierarchy). At the end of the fiber only an optical receiver and a fast D/A converter (DONU) are necessary for reconstructing the FDM signal [2, 3]. Usually, there is only one central head end supplying the digital FDM signal (DFDM). Fig. 1 gives an example of a fiber ring transmitting the DFDM signal from a central head end to several distribution areas.

In order to generate the DFDM signal, either a very fast A/D converter (ADC) can be employed to digitize the complete analog CATV signal or each baseband signal can be digitized separately using cost effective ADCs with relatively low sampling frequency and the FDM signal is generated using digital signal processing techniques.

In exisiting digital heads ends [3] all signal sources are shifted to IF using analog signal processing firstly and subsequently the IF signals are digitized in the head end individually. In order to convert the IF signals to channel-specific target frequencies the signals are fed into digital frequency converters (DFC) which are formed by digital complex filters, mixers and sample rate converters. In this way multi TV signals can be merged to a DFDM signal containing the entire analog CATV bandwidth [4].

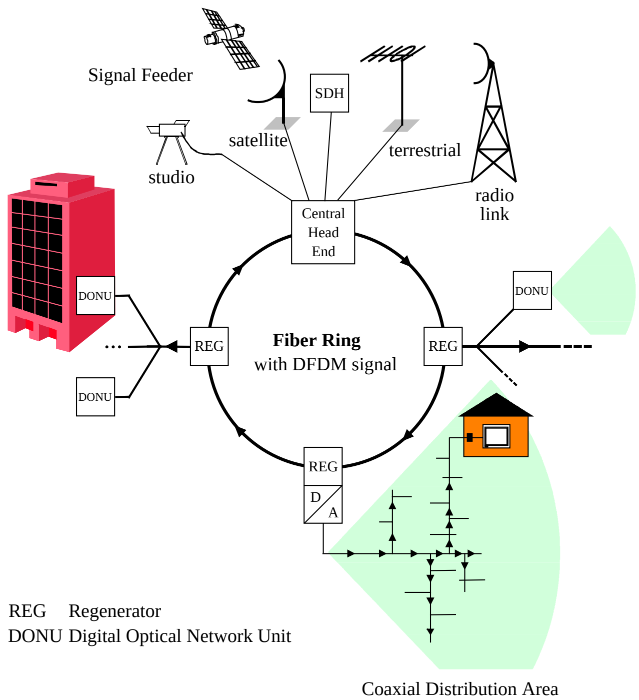

Fig. 1. Digital CATV network

Now, the challange is to design a completely digital intermediate frequency modulator (IFM) which converts the PAL or NTSC and associated audio baseband signals into the digital IF signal without using analog signal processing [5, 6]. This is the prerequisite to introduce an all digital transmission from the broadcasting studio to the vicinity of the subscribers. An effective solution is presented in this paper.

2. REQUIREMENTS

The following fundamental requirements have to be met by the IFM:

- Predistortion of the group-delay of the colour video blanking and synchronizing signal (CVBS signal) [7]
- Vestigial sideband modulation [7]
- An overall passband ripple of less than ±0.1 dB for the CVBS signal
- Unweighted Signal to noise ratio (SNR) for the video signal of more than 60 dB
- Preemphasis filter for the associated audio signals [7]
- Frequency modulation of the audio signals [7]
- SNR for the audio signal of more than 68 dB
- Output sampling frequency $f_S \approx 28.27$ MHz
- Spectrum of IF output signal centered at a quarter of the sampling frequency
- IF output signal compatible to the digital CATV distribution system described in [1, 2, 3, 4]
- Architecture with symmetric FIR filters suited for implementation with the ASICs described in [8]

The modulator presented herein is designed for TV signals according to the colour television standard PAL B/G [7] with two associated audio signals according to the ITU Rec. [9, 10]. However, the signal processing architecture for the CVBS signal is also suited for other colour television systems with a video bandwith equal or less than 5 MHz, e.g., the NTSC system. Since the IFM will be used for professional applications in the next generation digital TV distribution systems, the requirements given above are more stringent than those found in [7].

3. SIGNAL PROCESSING

The main building blocks of the IFM using complex signal processing are shown in Fig. 2. After clamping, amplifying and analog filtering, the CVBS signal is sampled with a relatively high sampling frequency f_S in order to reduce the requirements for the analog anti-aliasing lowpass filter. The resolution of 12 bits is sufficient to suppress effects caused by sampling with a frequency that is not an integer multiple of the TV line frequency as investigations of picture quality have shown. For PAL signals, mostly 13.5 MHz or 27 MHz is used for synchronous sampling. Considering the compatibility with the digital SDH transmission system mentioned in section 1, these sampling rates are not possible. Therefore f_S is derived from the clock frequency $f_{SDH} = 155.52$ MHz of the SDH transmission system according to $f_S \,/\, f_{SDH} = 2/11$. The sampling rate for the audio signals is $f_S/600 \approx 47$ kHz which is close to the 48 kHz standard for broadcasting studios. Therefore high quality low-cost ADCs can be used.

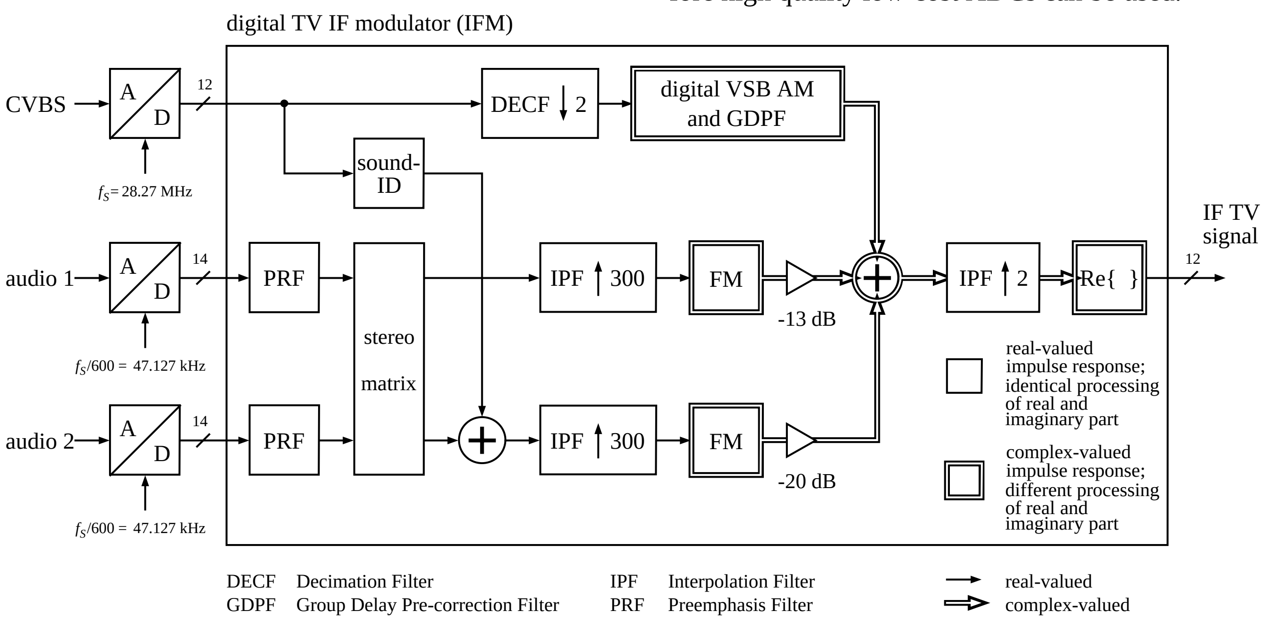

Fig. 2. Main building blocks of the digital IF modulator

For the video path in Fig. 2, the sampling frequency is first reduced by a decimation filter (DECF) in order to reduce the processing power needed for the following signal processing tasks. Subsequently the pre-correction of the group-delay (GDPF) and the vestigial sideband amplitude modulation (VSB AM) is carried out to the video signal. As a consequence of the ability of linear phase only FIR filters with mostly fixed point arithmetic are used in the IFM. For the VSB AM it is possible to suppress the lower sideband of the CVBS signal using a filter with complex-valued impulse response. An alternative solution with a real-valued impulse response is described later in subsection 3.1. The VSB amplitude modulator first inverts the CVBS signal, then it adds an offset and finally it implements a frequency-shifting using a complex mixer. In this way a negative VSB AM (C3F modulation) is achieved as required from [7].

The audio signal processing paths in Fig. 2 are nearly identical. The main tasks are preemphasis, sampling rate conversion and frequency modulation (FM). The audio signals are sampled with at least 14 bits/sample. In order to improve the SNR of the audio signal after demodulation a preemphasis filter (PRF) with a time constant of $\tau_P = 50\,\mu s$ increases the intensity of the higher spectral parts. There are three types of audio signals: mono, stereo and two-channel signals. A sound identification signal (sound ID) is added to audio signal 2. It depends on the ID whether the stereo matrix is active or not. The system B/G requires two sound carriers [9, 10]. Therefore both audio signals are frequency modulated separately. Before the FM, the sampling rate must be increased because the bandwidth is increased by the modulation. Also, an up-conversion by a factor 300 has to be performed to be able to add the FM audio signals to the video signal. It is not advantageous to carry out this conversion in one step. This is the reason why there are several stages performing the sampling rate conversion as described later. Now, both signals are fed into FM modulators. The center frequencies are adjusted so that the corresponding sound carriers are placed in defined distances to the vision carrier. In Fig. 2 the output of the modulators is a complex-valued signal and after an attenuation it is added to the modulated video signal. Finally an interpolation (IPF) is applied to the signal to return to the initial sampling frequency f_S and to compute the real-valued IF TV signal.

3.1. Video Signal Processing

This subsection deals with the architecture which is used to reduce the complexity and the amount of operations in the video path of the IFM. The structure is designed for an implementation with an application-specific integrated circuit (ASIC). This configurable ASIC contains several programmable FIR filters with symmetric impulse responses and a complex-valued

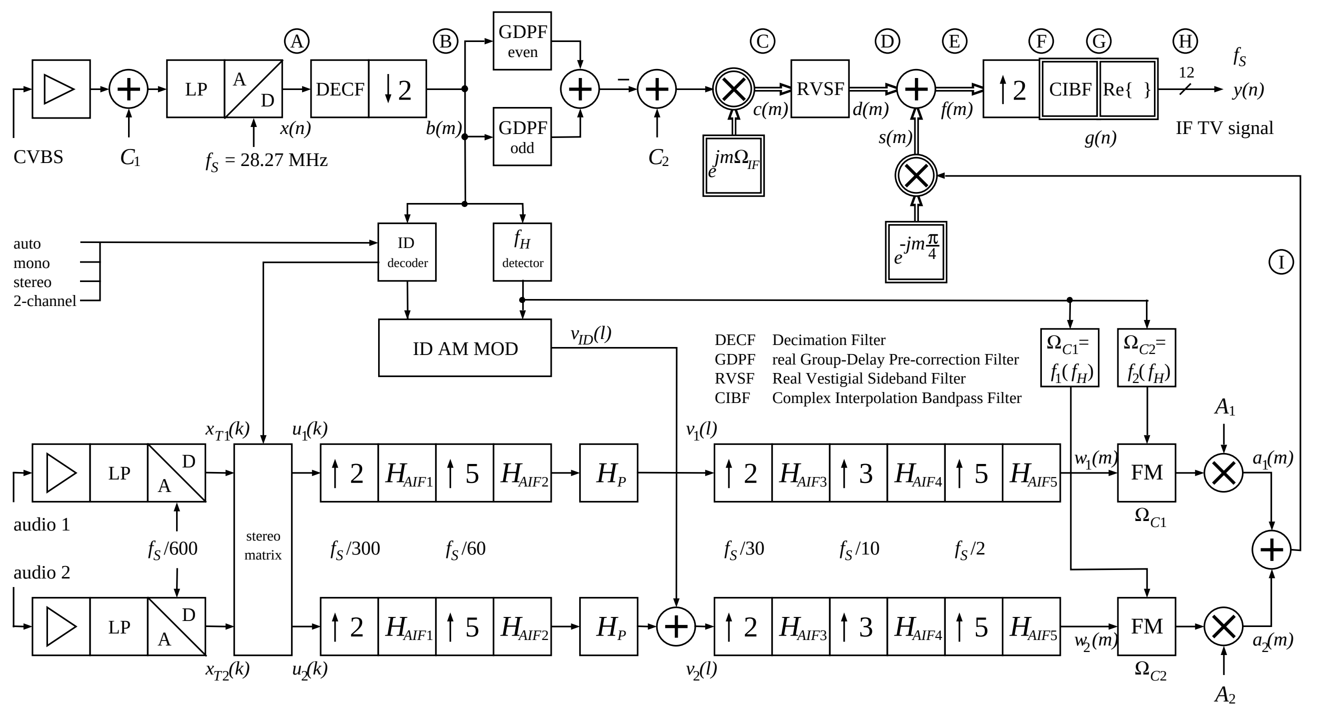

Fig. 3. Block diagram for the video and audio signal processing within the digital IF modulator

numerically controlled oscillator (NCO) [8]. Since these elements can be combined in several different ways, various signal processing tasks can be implemented. Fig. 3 shows the block diagram and Fig. 4 shows in principle the corresponding magnitude responses of the filters for the video signal.

An offset C_1 is added to the analog CVBS signal to adapt the signal to the dynamic range of the ADC. The decimation filter DECF and a downsampling by factor of two yields a decimation of the video signal. Due to the decimation a better arrangement of stopband, passband and transition ranges in the subsequent filters is achieved and the number of coefficients can be reduced. The *i*-th coefficient of the impulse response of a filter *x* is denoted as $h_x(i)$. The output signal is

$$b(m) = \sum_{i=0}^{N_{DECF}-1} h_{DECF}(i) \cdot x(2m-i). \tag{1}$$

m represents discrete time with the lower sampling frequency $f'_S = f_S/2$ while n corresponds to the higher sampling frequency f_S (Fig. 3). The *z*-transform of $x(n)$ and of the impulse response of the FIR filter $h_X(n)$ are given by

$$X(z) = \sum_{n=0}^{\infty} x(n) z^{-n} \quad \text{and} \quad H_X(z) = \sum_{n=0}^{N_X-1} h_X(n) z^{-n}. \tag{2}$$

with $z = e^{j\Omega}$, $\Omega = 2\pi f/f_S$. The corresponding transfer functions in Fig. 4 are given by

$$H'_X(f) = H_X\left(e^{j2\pi f/f_S}\right). \tag{3}$$

After some mathematical manipulations, the *z*-transform of $b(m)$ is

$$B(z') = \frac{1}{2}\sum_{\nu=0}^{1} X\left(z'^{\frac{1}{2}} W_2^{\nu}\right) \cdot H_{DECF}\left(z'^{\frac{1}{2}} W_2^{\nu}\right) \tag{4}$$

with $$W_2^{\nu} = e^{-j2\pi\nu/2} = e^{j\pi\nu} \tag{5}$$

where the variable in frequency domain $z' = z^2$ corresponds to the halved sampling frequency f'_S. The thick line in Fig. 5 shows the magnitude response of the implemented DECF. The coefficients are quantized with 16 bit each. The thin line indicates the ideal case without quantization. The tolerance scheme is given by the shaded area. The stopband attenuation is greater at the positions where the main spectral parts of the luminance and chrominance signal occur after decimation. The passband ripple, which is only about ±0.02 dB, is shown enlarged in a subwindow.

The next processing task in Fig. 3 is the pre-correction of the group-delay with an FIR filter (GDPF) which has an asymmetric impulse response due to the fact that it has no constant group-delay. In order to implement the GDPF with the same ASICs used for all other symmetric filters the impulse response is split into its even and odd part. If the symmetric property of the two partial impulse responses is used to reduce the number of multiplications in each partial filter then the

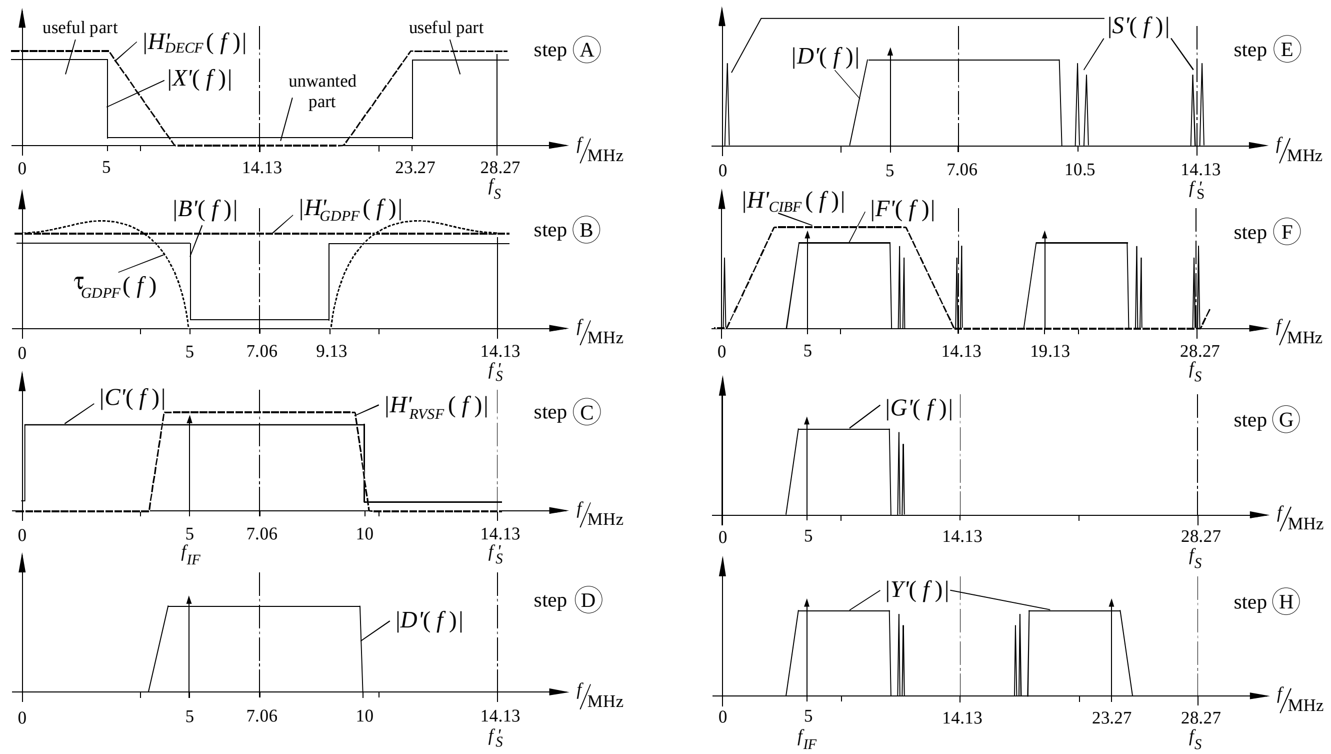

Fig. 4. Video signal processing within the digital IF modulator in frequency domain (principles); symbols correspond to (3)

total number of multiplications in the entire filter is equal to the number of coefficients in the GDPF. For this reason the split of the GDPF in even and odd part causes almost no additional computational overhead. The design of the GDPF will be discussed in subsection 3.2. The magnitude response in dB and the group-delay τ_{GDPF} in ns is shown in Fig. 6. The group-delay is compliant to the tolerance scheme given in [7] (curve B). Combining the DECF and the GDPF in a single asymmetric filter would require a considerably higher number of coefficients. Fig. 6 shows an increase of the magnitude response outside the passband. This is an effect caused by the design process of the filter and the maximal number of available coefficients. Nevertheless the overall magnitude response of the entire IFM is within the given tolerance scheme as will be shown in section 5, Fig. 17.

In order to perform a negative vestigial sideband modulation the signal has to be inverted and scaled. A detailed investigation, which is not shown here, results in a scaling factor x and the offsets C_1 and C_2 to be

$$C_1 = 0.265 \cdot s_M \,,\; C_2 = 0.508 \cdot y_2 A \,,\; x = -0.616 \cdot \frac{y_2}{y_1} \,. \quad (6)$$

s_M is the maximum signal level of the CVBS signal (133% of the white level). A denotes full scale. The maximum signal level before scaling is $y_1 A$ and the maximum signal level after scaling is $y_2 A$. The scaling by factor x can be done easily by modifying the coefficients of the GDPF. Simulation of the IFM has shown that a maximum SNR is achieved if

$$20 \lg y_1 \approx -1 \,\mathrm{dB} \text{ and } 20 \lg y_2 \approx -3 \,\mathrm{dB} \quad (7)$$

are used. The frequency-shifting is now done with the help of a complex-valued carrier that is provided by a numerical oscillator with the specific frequency

$$\Omega_{IF} = 2\pi \cdot 4.994 \,\mathrm{MHz} / f_S' \,. \quad (8)$$

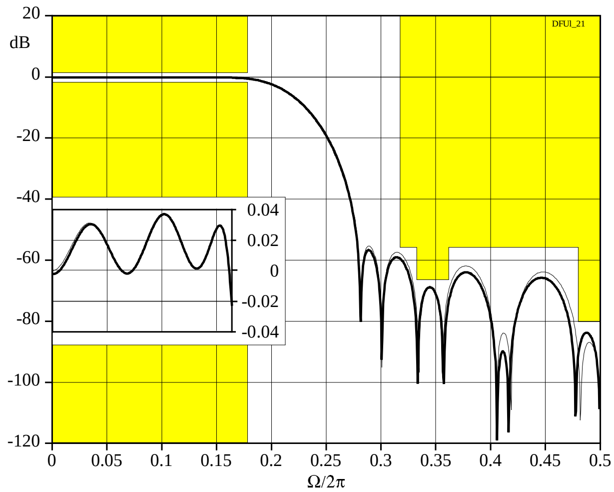

Fig. 5. DECF with 28 coefficients

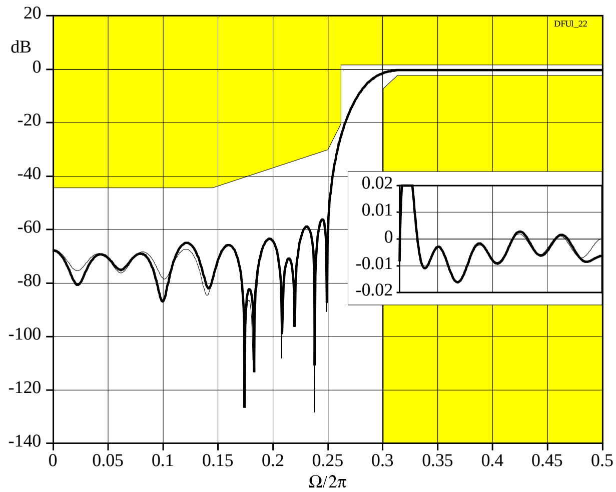

Fig. 7. RVSF with 51 coefficients

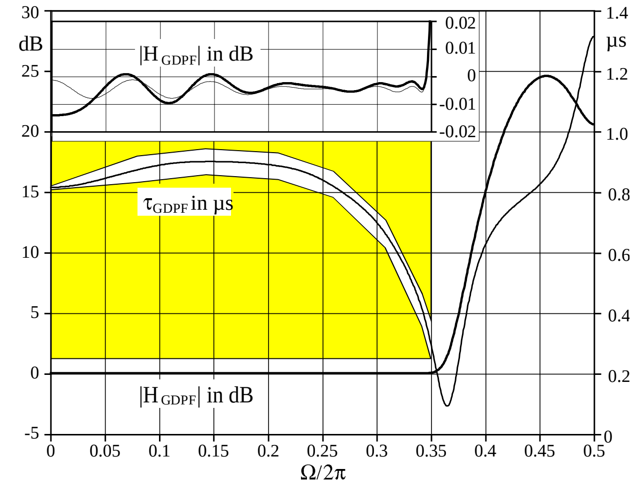

Fig. 6. GDPF with 24 coefficients

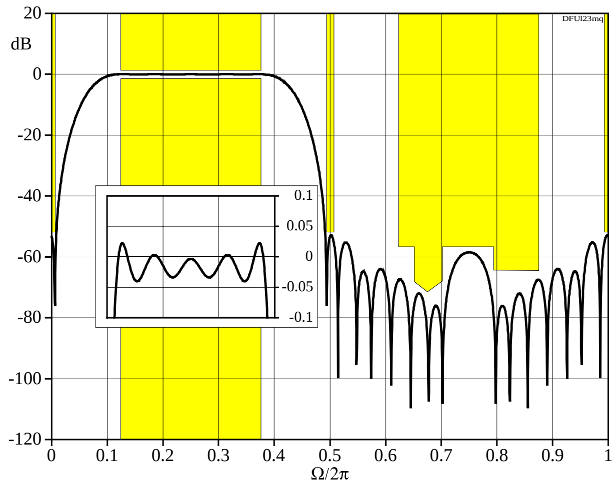

Fig. 8. CIBF with 27 coefficients

The specifications for the vestigial sideband filter in [7] allow the combination of the requirements in the tolerance scheme for the lower and upper edge frequencies of the asymmetric bandpass filter in a tolerance scheme for a symmetric bandpass filter. In the discrete time domain a highpass filter can also fulfill the function of this specific bandpass filter. The carrier frequency in (8) is chosen to place the signal spectrum at a position where the real vestigial sideband filter (RVSF) can be a simple highpass filter with real coefficients as shown in Figs. 3, 4C and 7, so that the same hardware that is also suited for processing complex-valued signals can be used for the DECF, GDPF and RVSF.

In Fig. 3 the FM sound signal $s(m)$ which is discussed in subsection 3.3 is added. The magnitude response of $S'(f)$ is shown in Fig. 4E. $S'(f)$ also contains spectral parts near f_S' and $f=0$. These parts have a maximum distance to the spectrum of the video signal $D'(f)$ centered at $f_S'/2$. The resulting signal is

$$f(m) = s(m) - \sum_{l=0}^{N_{RVSF}-1} \left\{ \left\{ \sum_{i=0}^{N_{DECF}-1} \sum_{k=0}^{N_{GDPF}-1} h_{DECF}(i)\, h_{GDPF}(k)\, h_{RVSF}(l)\, x\big(2(m-k-l)-i\big) \right\} - C_2 \cdot h_{RVSF}(l) \right\} e^{j(m-l)\Omega_{IF}} . \qquad (9)$$

Applying the corresponding comb function (as shown below)

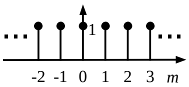

$$K\left(e^{j\Omega'}\right) = 2\pi \sum_{\mu=-\infty}^{\infty} \delta(\Omega' - 2\pi\mu) \qquad (10)$$

to (9), the TV signal $f(m)$ can be written in frequency domain

$$\begin{aligned} F(z')\big|_{z'=e^{j\Omega'}} = \\ S(z') + H_{RVSF}(z') \cdot \Big\{ C_2 K\left(z' \cdot e^{-j\Omega_{IF}}\right) - \\ B\left(z' \cdot e^{-j\Omega_{IF}}\right) \cdot H_{GDPF}\left(z' \cdot e^{-j\Omega_{IF}}\right) \Big\} \Big|_{z'=e^{j\Omega'}} \end{aligned} \qquad (11)$$

where $\Omega' = 2\pi\, f / f_S'$. Finally an interpolation by a factor of two is applied to the signal $f(m)$ to return to the initial sampling frequency f_S and to compute the real-valued IF TV signal (Fig. 3). As the video signal was frequency-shifted with (8), its spectrum is centered around ¼ f_S after interpolation. The interpolation filter (CIBF) must be a bandpass filter to select the spectral parts centered at ¼ f_S. At the same time, the undesired parts of the sound signals at ½ f_S and $f=0$ must be attenuated (see Figs. 4F and 8). Since the impulse response of the CIBF is complex-valued, a convolution of two complex-valued signals must be carried out. Normally this requires four real-valued convolutions simultaneously. However, if an FIR filter is used that has the following properties:

- magnitude response with symmetry about the axes at ¼ f_S and ¾ f_S (Fig. 8),
- odd number of coefficients,
- linear phase,
- interpolation by factor two,
- only real-valued output,

then the CIBF can be split into two polyphases $h_0(m)$ and $h_1(m)$ with real-valued symmetric impulse responses as shown in Fig. 9. Only one filter operation for each output sample must be computed and the polyphases $y_0(m)$ and $y_1(m)$ of the output signal $y(n)$ can be computed at the lower sampling frequency f_S'. Thus,

$$\begin{aligned} y_0(m) &= j \sum_{\nu=0}^{\frac{N_{CIBF}-1}{2}} \mathrm{Im}\{ f(m-\nu) \} \cdot h_0(\nu) \\ y_1(m) &= \sum_{\nu=0}^{\frac{N_{CIBF}-3}{2}} \mathrm{Re}\{ f(m-\nu) \} \cdot h_1(\nu) \end{aligned} \qquad (12)$$

and $y(2m+l) = y_l(m)$, m integer, $l = 0, 1$. (13)

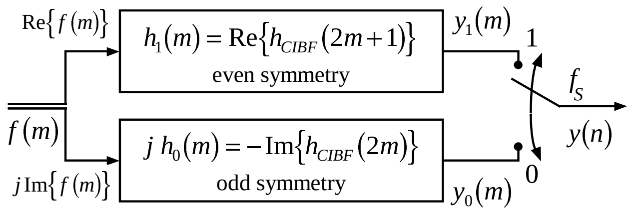

Fig. 9. Filter structure for the CIBF if $(N_{CIBF}-1)/2$ is odd

In the frequency domain, we obtain for the complex-valued signal after interpolation

$$G\left(e^{j\Omega}\right) = F\left(e^{j2\Omega}\right) \cdot H_{CIBF}\left(e^{j\Omega}\right) . \qquad (14)$$

Therefore, the spectrum of the real-valued IF signal is

$$Y\left(e^{j\Omega}\right) = \frac{1}{2}\left(G\left(e^{j\Omega}\right) + G^{*}\left(e^{-j\Omega}\right) \right) . \qquad (15)$$

The magnitude response is shown in Fig. 4H. For further processing of $y(n)$ either the spectral part in original or in mirrored position can be used.

3.2. Design of the GDPF

Whereas the DECF, the RVSF and the CIBF with constant group-delay can be designed applying the well-known method of Parks/McClellan, the GDPF necessitates another design method. As generally known, the relation between the group-delay $\tau(\Omega)$ and the phase

$\varphi(\Omega) = \operatorname{arc} H(\Omega)$ of the transfer function $H(\Omega)$ is given by

$$\varphi(\Omega) = -\int \tau(\Omega)\, d\Omega + \Phi \qquad (16)$$

where Φ is a constant that is used to obtain a causal impulse response. Let $H(\Omega)$ be specified by a vector of M complex values in the frequency range of interest. Then

$$\mathbf{H} = \begin{bmatrix} H_0 & H_1 & \dots & H_{M-1} \end{bmatrix}^T \text{ with} \qquad (17)$$

$$H_i = \left|H(\Omega_i)\right| \cdot e^{j\varphi(\Omega_i)} \;,\; \Omega_i = 2\pi \frac{f_i}{f_S} \quad i = 0 \dots M-1 . \qquad (18)$$

The task is to approximate $H(\Omega)$ by an FIR filter with N coefficients. The transfer function $I(\Omega)$ of this filter is determined at the M ($M > N$) frequency points of interest by

$$\mathbf{I} = \begin{bmatrix} I_0 & I_1 & \dots & I_{M-1} \end{bmatrix}^T \qquad (19)$$

with $$I_i = \sum_{n=0}^{N-1} h_n \cdot e^{-jn\Omega_i} \quad i = 0 \dots M-1 . \qquad (20)$$

The approximation error is defined as

$$\mathbf{e} \equiv \mathbf{I} - \mathbf{H} . \qquad (21)$$

If $\mathbf{I}$ is written in matrix form, i.e.,

$$\mathbf{I} = \mathbf{W} \cdot \mathbf{h} \text{ with} \qquad (22)$$

$$\mathbf{W} = \begin{bmatrix} 1 & e^{-j\Omega_0} & \dots & e^{-j(N-1)\Omega_0} \\ 1 & e^{-j\Omega_1} & \dots & e^{-j(N-1)\Omega_1} \\ \dots & \dots & \dots & \dots \\ 1 & e^{-j\Omega_{M-1}} & \dots & e^{-j(N-1)\Omega_{M-1}} \end{bmatrix} \text{ and } \mathbf{h} = \begin{bmatrix} h_0 \\ h_1 \\ \dots \\ h_{N-1} \end{bmatrix}$$

the following system of linear equations is obtained

$$\mathbf{e} = \mathbf{W} \cdot \mathbf{h} - \mathbf{H} . \qquad (23)$$

A good approximation is achieved by solving

$$e_{\min} = \min_{\mathbf{h}} \left\{ \mathbf{e}^* \mathbf{e} \right\} = \min_{\mathbf{h}} \left\{ (\mathbf{W} \cdot \mathbf{h} - \mathbf{H})^* \cdot (\mathbf{W} \cdot \mathbf{h} - \mathbf{H}) \right\} \qquad (24)$$

where '*' denotes the complex conjugated and transposed matrix or vector, respectively. With the matrix

$$\mathbf{R} = \mathbf{W}^* \cdot \mathbf{W} = \mathbf{R}^* , \qquad (25)$$

we obtain from (24)

$$\begin{aligned} e_{\min} = \min_{\mathbf{h}} \Big\{ & \mathbf{H}^*\mathbf{H} - \mathbf{H}^*\mathbf{W}\mathbf{R}^{-1}\mathbf{W}^*\mathbf{H} \\ & + \left(\mathbf{W}^*\mathbf{H} - \mathbf{R}\mathbf{h}\right)^* \mathbf{R}^{-1} \left(\mathbf{W}^*\mathbf{H} - \mathbf{R}\mathbf{h}\right) \Big\} \end{aligned} \qquad (26)$$

which can be proven using $(\mathbf{X} \cdot \mathbf{Y})^* = \mathbf{Y}^* \cdot \mathbf{X}^*$. Since $e_{\min}$ is always positive the minimum is given by setting the quadratic term in (26) containing $\mathbf{h}$ to zero. This yields

$$\mathbf{h} = \left(\mathbf{W}^* \cdot \mathbf{W}\right)^{-1} \cdot \mathbf{W}^* \cdot \mathbf{H} . \qquad (27)$$

The resulting transfer function $I(\Omega)$ depends on the proper selection of the arrangement of the M frequency points. The result which meets the requirements in [7] is shown in Fig. 6.

3.3. AUDIO SIGNAL PROCESSING

The audio signal processing will now be discussed in detail for one audio channel. In the case of a stereo signal the stereo matrix computes the signals

$$\begin{aligned} u_1(k) &= \tfrac{1}{2}\left(x_{T1}(k) + x_{T2}(k)\right) \\ u_2(k) &= x_{T2}(k) \end{aligned} \qquad (28)$$

where $T1$ denotes the left channel and $T2$ the right channel. In case of a mono or two-channel signal $u_i(k) = x_{Ti}(k)$ holds. The operating mode for the stereo matrix is determined by the ID decoder which extracts the information out of the tele text line in the video signal. Otherwise it is user defined.

In Fig. 3 various stages for the sampling rate conversion to f_S' are presented. The total interpolation factor of 300 is split into its prime factors. This enormously reduces the number of coefficients and the number of operations per clock cycle as well. The first anti-imaging filter (AIF1) is a halfband filter with 23 coefficients. The AIF2 is a fifth-band filter where every fifth coefficient is zero except for the middle coefficient. The magnitude response is shown in Fig. 10. This kind of filter can be implemented using the structure shown in Fig. 11 with high efficiency. The values for the multipliers in the filter structure are derived from the filter coefficients according to [11]. AIF3, AIF4 and AIF5 have 15 coefficients each.

The analog preemphasis filter with

$$H_{P,a}(\omega) = 1 + j\omega\tau_P \qquad (29)$$

is excellently approximated in the z domain by

$$H_P(z'') = H_{P1} \cdot H_{P2} = a\left(1 + bz''^{-1}\right) \cdot \frac{1 + z''^{-1}}{1 - cz''^{-1}} \qquad (30)$$

where $z'' = z^{60}$ corresponds to the sampling frequency of $f_S/60$. H_P is placed behind the second interpolation stage considering that the implementation of the preemphasis filter is less complex if the sampling frequency is about 10 times higher than the initial sampling frequency of the audio signal (Fig. 12). H_{P1} implements the preemphasis and H_{P2} compensates the increasing of the magnitude response of H_{P1} at frequencies higher than the audio frequencies. Fig. 13 shows the magnitude

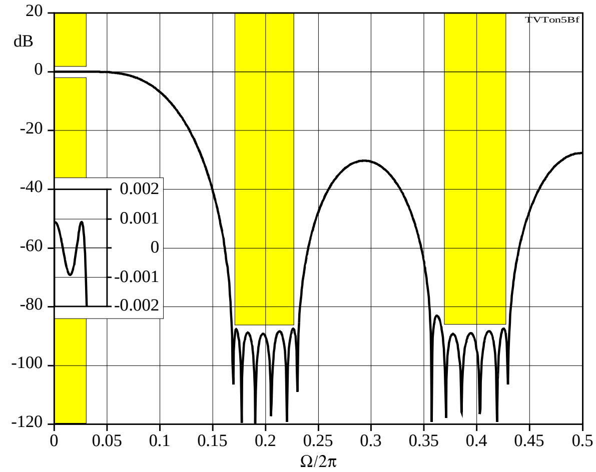

Fig. 10. Magnitude response of fifth-band filter AIF2

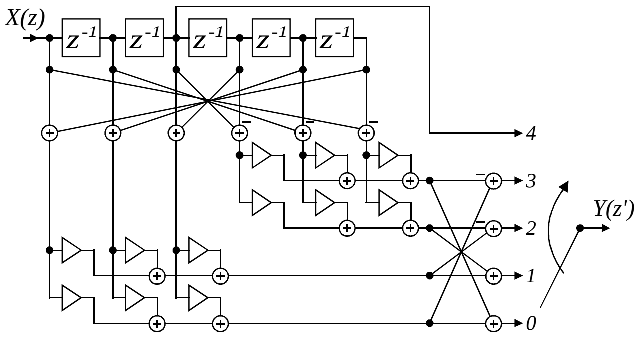

Fig. 11. Polyphase fifth-band filter AIF2 with 29 coefficients

responses of AIF1, AIF2, H_{P1}, H_{P2} and the total magnitude response

$$H_T(z'') = H_{AIF1}\left(z''^5\right) \cdot H_{AIF2}\left(z''^2\right) \cdot H_P(z''). \qquad (31)$$

Now, a sound identification signal $v_{ID}(l)$ is added to the signal $v_2(l)$ in order to identify the type of the audio signals mentioned above for the TV receivers. $v_{ID}(l)$ is an amplitude modulated carrier with a carrier frequency of $3.5 f_H$. It is locked to the horizontal line frequency f_H using a line frequency detector. The generation of $v_{ID}(l)$ is described in detail in [6]. After this, the sampling frequency is increased in 3 stages by the filters AIF3, AIF4 and AIF5 similar to AIF1 and AIF2.

As is well-known, the FM is achieved by manipulating the phase increment of the digital oscillator every clock cycle by the signal $w_x(m)$, x = 1, 2. The frequency swing of 50 kHz is adjusted by scaling the coefficients in the AIF5. The FM signals $a_x(m)$ are attenuated by multiplication with the constants A_x, x = 1, 2, to achieve the desired level of the sound carriers [9]. As is recommended in [10] the sound carrier frequencies Ω_{C1} and Ω_{C2} are locked to the line frequency f_H.

Since the signals $a_x(m)$ are real-valued, it is impossible to carry out the FM with the desired sound carrier frequencies of about 10.5 MHz that are shown in Fig. 4E directly. This is, because the mirrored spectral parts would overlap with the spectrum of the video signal. For this reason the two real-valued frequency-modulated sound signals are placed at intermediate frequencies f_x which are 1/8 of the actual sampling frequency f_S' away from this sound carriers (Fig. 14). These specific intermediate frequencies are chosen because the mirrored spectral parts of the real-valued sound signals are placed at positions where the distance from the spectrum of the video signal is maximal after the frequency-shifting according to (32) (Fig. 4E). As a consequence, the transition ranges of the following CIBF that eliminates the mirrored spectral parts are maximally wide (Fig. 4F).

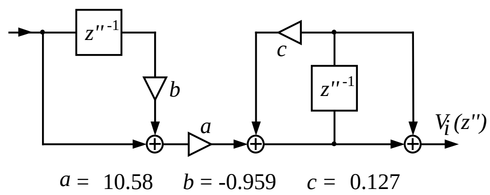

Fig. 12. Structure of the preemphasis filter

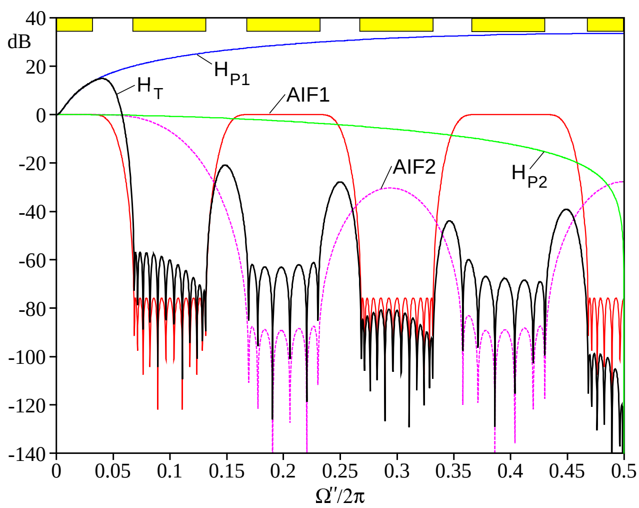

Fig. 13. Magnitude responses of filters for audio processing. Top: schematic representation of upsampled audio spectrum

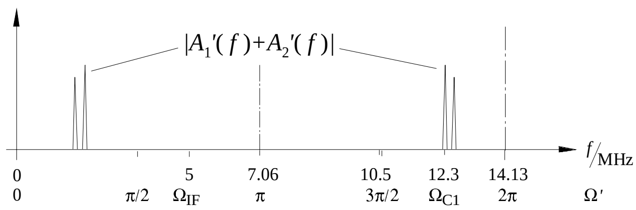

Fig. 14. Spectrum of the real-valued FM signals

$$s(m) = \left[a_1(m) + a_2(m)\right] \cdot e^{-jm\pi/4} \qquad (32)$$

The frequency-shift is carried out with the structure in Fig. 15 which needs only one multiplier, an inverter and few multiplexers. It can easily be implemented with an FPGA. Since the signal $s(m)$ is clipped to a word length of 12 bits/sample before adding to the modulated video signal, the SNR is almost only limited by this clipping and not by the noise produced during audio signal processing.

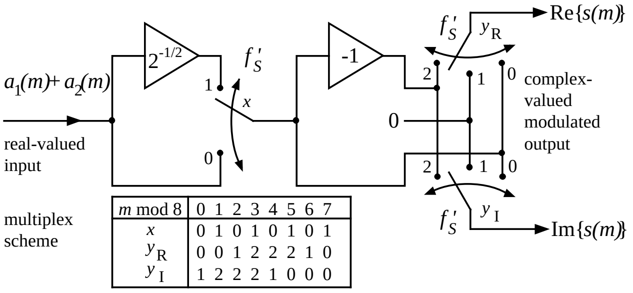

m mod 8	0 1 2 3 4 5 6 7
x	0 1 0 1 0 1 0 1
y_R	0 0 1 2 2 2 1 0
y_I	1 2 2 2 1 0 0 0

Fig. 15. Mixer for sound signals

4. Implementation

In this section a hardware structure that is suited for the realization of the IFM is described briefly. Fig. 16 shows the simplified block diagram of the digital part of the IFM hardware which consists of two different ASICs A and B [8], two FPGAs and a floating-point DSP. Type A of the ASIC is employed three times for different signal processing tasks. The left part describes the audio signal processing whereas the right part of the block diagram describes the video signal processing. One ASIC of type A can carry out two separate FIR filter operations for real-valued or complex-valued signals and either frequency-shifting or frequency modulation at the same time. An ASIC of type B is employed for the three interpolation stages with the factors two, three and five from 471 kHz to 14.13 MHz of both audio channels. Even and odd parts of the GDPF are located in separate ASICs. The RVSF with 51 coefficients utilizes all FIR filters in the ASIC A3 simultaneously. Consequently, all three parts in ASIC A3 are used for signal processing, too. According to Fig. 11, the CIBF is split internally into its real and imaginary part of the impulse response. All ASICs have a word length of 15 bits for the output signal, up to 19 bits for the internal signals and 16 bits for the coefficients. Since these ASICs have been specifically designed for the DFC in the CATV head end some simple operations necessary for implementation of the IFM cannot be carried out by the ASICs themselves. These additional operations located in the FPGAs are mainly additions, multiplications with a constant, and multiplex functions.

5. Performance

If the symmetry of the filters is considered, the total number of multiplications and additions per clock cycle $1/f_S$ for video signal processing is 61 and 115, respectively. This results in a total of 4.9 billon operations per second (GOPS). The audio signal processing requires about 7 multiplications and 7 additions in each clock cycle $1/f_S$. The total is 0.4 GOPS which is about 7% of the total processing power. The overall magnitude response for the video signal is shown in Fig. 17 (bottom). Due to the null in the magnitude response at the vision carrier frequency of the image part the vision carrier from the image part is totally attenuated after interpolation with the CIBF. The passband ripple is ±0.02 dB if the complex-valued IF TV signal $g(n)$ is looked at behind the CIBF. It is only the number of co-

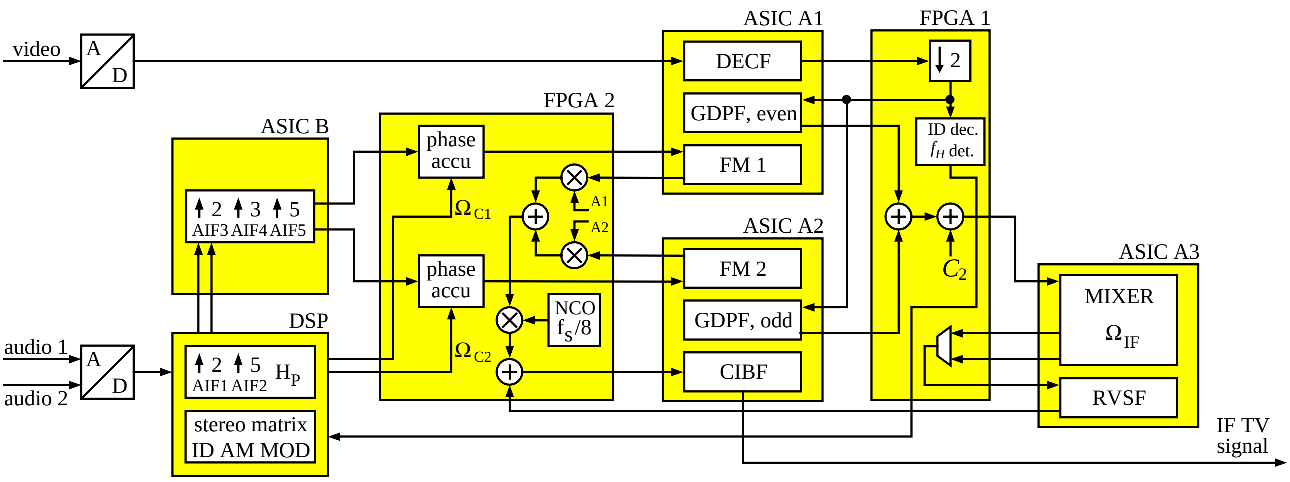

Fig. 16. Simplified block diagram of DBM hardware

efficients that limits the passband ripple of the IFM. The simulated signal spectrum is shown in Fig. 17 (top). A weighted SNR of 77 dB is achieved for the video signal and an average weighted THD+N of 85 dB is achieved for the audio signals one and two (Fig. 18) [6, 12]. Fig. 19 shows the step response of the video path for a step with 200 ns rising time and the tolerance scheme given in [13].

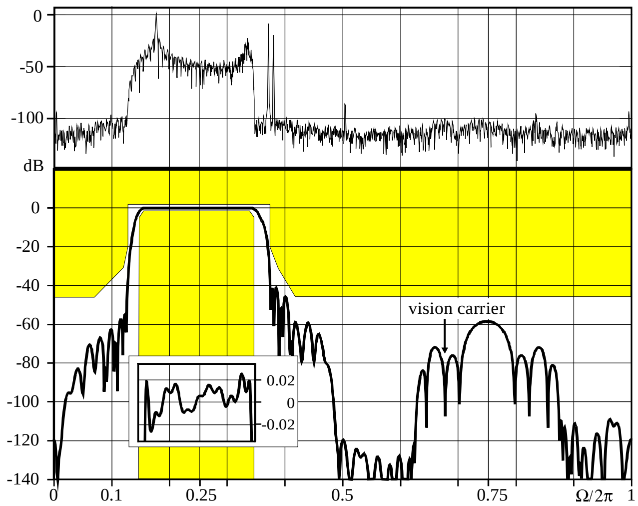

Fig. 17. TV IF signal spectrum including sound (top), overall magnitude response for the video signal (bottom)

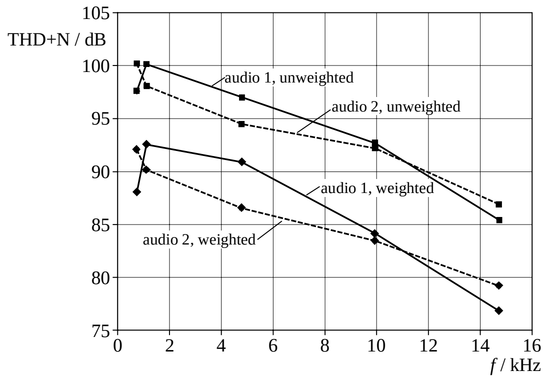

Fig. 18. Total harmonic distortion and noise for the audio signals

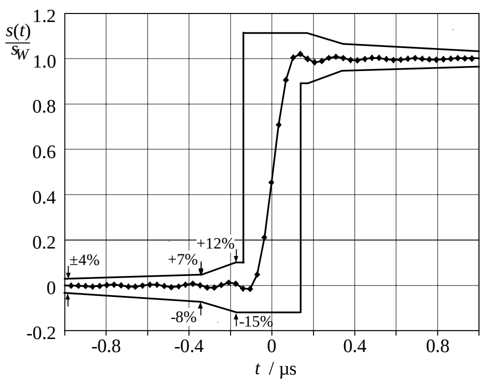

Fig. 19. Step response of the video path

6. Conclusion

This paper presents an efficient method for the conversion of conventional CVBS video signals with two associated audio signals into a high quality digital IF TV signal using digital signal processing techniques. It is shown that all required filter operations can be carried out with identical FIR filter structures that have a symmetrical impulse response to simplify the hardware complexity. The IFM requires low processing power and is well suited for implementation with ASICs. In addition, the achieved overall passband ripple of less than ±0.02 dB is better than required in the ITU specification. The proposed system architecture is paving the way for all-digital CATV transmission systems and "software head ends" for distributing conventional TV signals from the studio to the subscribers.

Acknowledgement

The authors would like to express their sincere thanks to the Bosch Telecom company.

References

[1] W. Bambach, K. Grotz, "First installation of a novel all-digital access network system for distributive and interactive services", Optoelectronics and Communications Conference, Tokyo, 1996.

[2] W. Bambach, G. Berthes, H. Lohscheller, J. Mayer, "Digital optical trunk system for CATC networks", International Television Symposium Montreux, 1997.

[3] H. Feilhauer, K. Grotz, J. Speidel, "All digital optical CATV distribution system", Proc. ITG-Workshop Optische Teilnehmerzugangsnetze, Dresden, 1995.

[4] H. G. Göckler, K. Grotz, "Diamant - All digital frequency division multiplexing for 10 Gbit/s fibre-optic CATV distribution systems", European Signal Processing Conference (EUSIPCO), Edinburgh, pp. 999-1002, 1994.

[5] D. Wenzel, J. Speidel, "A digital IF modulator for video and associated audio signals", Proc. IEEE International Conference on Communications (ICC), Vancouver, June 1999, pp. 1010-1016.

[6] D. Wenzel, "A digital TV and audio modulator for digital broadband distribution networks", Dissertation, University of Stuttgart, 1999.

[7] ITU-R Rec. BT.470-5, "Conventional television systems", Genf, 1998.

[8] "ASICs DFUlong and DFUint, Documentation", Bosch Telecom, Backnang, 1997.

[9] ITU-R Rec. BS.707-3, "Transmission of multisound in terrestrial television systems PAL B, G, H and I", Genf, 1998.

[10] ITU-R Rec. BS.795-3, "Transmission of two or more sound programs or information channels in television", Genf.

[11] Z.-J. Mou, “Symmetry exploitation in digital interpolators/decimators”, IEEE Transactions on Signal Processing, Vol. 44, no. 10, pp. 2611-2619, Oct. 1996.
[12] ITU-R Rec. BS.468-4, “Measurement of audio-frequency noise voltage level in sound broadcasting”, Genf, 1986.
[13] ITU-T Rec. J.61, “Transmission performance of television circuits designed for use in international connections”, Genf, 1990.

Dietmar Wenzel was born in Waiblingen, Germany, in 1968. He received his Dipl.-Ing. and Dr.-Ing. degree in Electrical Engineering from the University of Stuttgart, Germany in 1994 and 1999. Since 1994 he has been with the Institute of Telecommunications at the University of Stuttgart as a research and teaching assistant. At the same time he has been closely cooperating with the development division for digital broadband communications systems at Bosch Telecom Backnang. His research interests include digital signal processing with a focus on interfaces for broadband communications systems and sample rate conversion.

Joachim Speidel studied Electrical Engineering at Stuttgart University and received his Dipl.-Ing. and Dr.-Ing. degree in 1974 and 1980. In 1980 he joined Philips as an R & D engineer to work on video data compression, Cable Television, ISDN, optical communications and local loop systems. He as been engaged in various international positions, finally as a Director for R & D. Since 1992, Dr. Speidel is Professor and Director of the Institute of Telecommunications at Stuttgart University. His main research areas are multimedia communication systems, mobile communications and video coding.